

## **Subsecond Measurements of the Optical Properties in the Spectral Range 0.4–1.1 $\mu\text{m}$ Near High-Temperature Transformations of Samarium Oxide<sup>1</sup>**

**T. P. Salikhov<sup>2</sup> and V.V. Kan<sup>2</sup>**

---

A new dynamic method is described for measuring the spectral directional-hemispherical reflectivity in the spectral range 0.4–1.1  $\mu\text{m}$  near high-temperature phase transformations of refractory materials. The use of diffuse sample irradiation enables one to exclude the influence of an abrupt variation of the angular reflection distribution of sample surface at the phase transitions. The experimental results on samarium oxide showed that light pulses are emitted by the sample during the high-temperature transformations.

---

**KEY WORDS:** optical properties; phase transformation; polychromatic diffuse irradiation; reciprocity principle; samarium oxide; spectral reflectance; transformation temperature.

### **1. INTRODUCTION**

The study of spectral reflectivity in the region of high-temperature phase transformations of the refractory materials is complicated. The sharp change in angular reflection distribution at the transition point complicates the problem of collecting the radiation reflected from the sample to the hemisphere. In this case, the method of integrating sphere for collecting the reflected radiation is not adequate as it is suitable for materials having a diffusely reflecting surface [1].

In the present work, a new dynamic method for measuring the spectral directional-hemispherical reflectivity near the high-temperature phase

---

<sup>1</sup> Paper presented at the Third Workshop on Subsecond Thermophysics, September 17–18, 1992, Graz, Austria.

<sup>2</sup> Academy of Sciences, Physical Technical Institute, Timiryazeva 2B, 70084 Tashkent, Republic of Uzbekistan.

transformation of refractory materials is described. In order to eliminate the influence of the sharp change in the angular reflection distribution of sample surface at the transition point, we used a diffuse hemispheric irradiation of the sample. It enables one to measure the spectral reflectivity for any kind of sample, regardless of the sample texture [2, 3].

By means of this new experimental technique, the normal spectral reflectivity and emissivity of samarium oxide near and at the point of high-temperature transformations ( $> 2000$  K) were measured in the wavelength range  $0.4\text{--}1.1\ \mu\text{m}$ . The transformation temperatures of  $\text{Sm}_2\text{O}_3$  were also obtained.

## 2. METHOD AND APPARATUS

According to Helmholtz's reciprocity principle, the reflectance for a given angle of incidence is equal to the radiance factor for uniform hemispherical irradiation of the sample with collection of reflected radiation at the same angle. Therefore, the spectral directional-hemispherical reflectance can be determined indirectly by measuring the spectral radiance

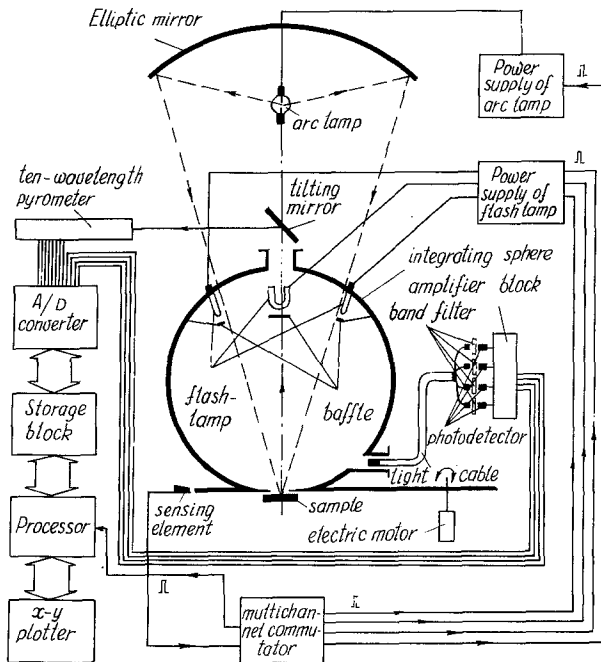


Fig. 1. Schematic diagram of the experimental system.

factor using diffuse irradiation of the sample [4]. For this purpose, flash-lamps are placed in the integrating sphere and they irradiate the sample surface heated by an imaging furnace. Figure 1 shows a schematic diagram of the experimental system. The sample placed at the focal zone of an imaging furnace is heated to temperatures above its melting point. Then the sample surface is rapidly covered by the integrating sphere for 20 ms and the sample is allowed to cool. A multichannel commutator starts the recording system and turns on the flash-lamps at the desired time.

The integrating sphere (150 mm in diameter), with a uniform diffuse high reflectance, has three apertures in the wall for sample irradiation, pyrometer, and control channel outputs. Three flash-lamps, placed in the integrating sphere, are activated successively. The time interval between the activations of the flash-lamps is regulated by the multichannel commutator. The time diagram of the starting pulses is shown in Fig. 2. The flash-lamps produce a diffuse irradiation of the cooling sample at the moment of the phase transition of interest through the lower aperture in the sphere wall (5 mm in diameter). The reflected portions of the polychromatic light incident on the sample and temperature signals during the sample cooling are measured by means of a 10-wavelength high-speed micropyrometer that operates in the spectral range 0.4–1.1  $\mu\text{m}$ . The viewing spot of the pyrometer on the sample is 0.5 mm in diameter.

Figure 3 shows a typical record for  $\text{Sm}_2\text{O}_3$  during the sample cooling stage. The curves have four peaks that correspond to the phase transitions

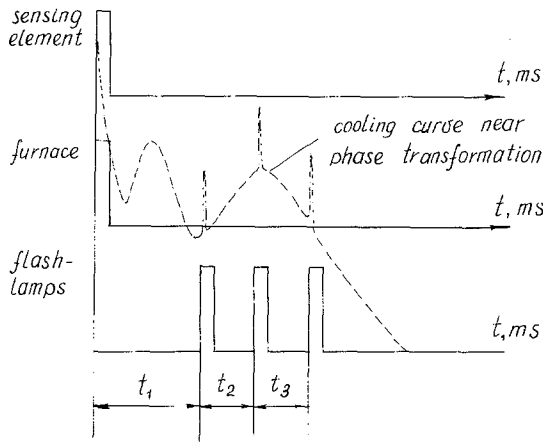
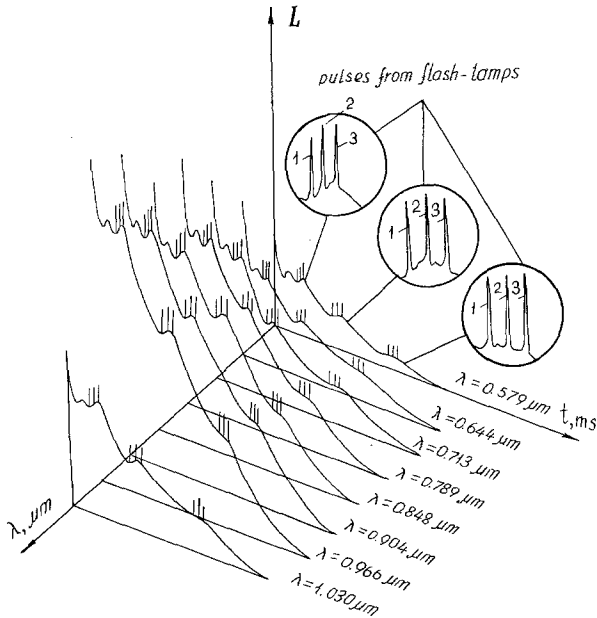


Fig. 2. Time diagram of the starting pulses of the multi-channel commutator.

of  $\text{Sm}_2\text{O}_3$ . These peaks are “bombarded” by the pulse light of the flash-lamps.

The light pulses reflected from the sample surface through the upper hole in the sphere wall enter the optical system of the pyrometer (see Fig. 4). Spectral decomposition of the light flux reflected from the sample is carried out by a diffraction grating. The diffracted rays are then focused by the lens on the set of 10 detectors. The electrical signals from the detectors are finally amplified and recorded. The pyrometer is working in the spectral range  $0.4\text{--}1.1\ \mu\text{m}$  and in the temperature range  $1300\text{--}3000\ \text{K}$ . The pyrometer was calibrated with a gas-filled tungsten ribbon-lamp at  $0.65\ \mu\text{m}$ . Calibration values of the radiance temperatures for other wavelengths were obtained using the data of Latyev et al. [5] on the monochromatic emissivity of tungsten. The calibration uncertainty of the radiance temperatures was less than  $1.5\ \text{K}$  at  $2000\ \text{K}$  and at wavelengths of  $0.644, 0.713, 0.789, 0.848, 0.904,$  and  $0.966\ \mu\text{m}$ .



**Fig. 3.** Typical cooling curves of the sample “bombarded” near phase transitions by radiation from flash-lamps.  $L$ ,  $\lambda$ , and  $t$  are radiance, wavelength, and time, respectively.

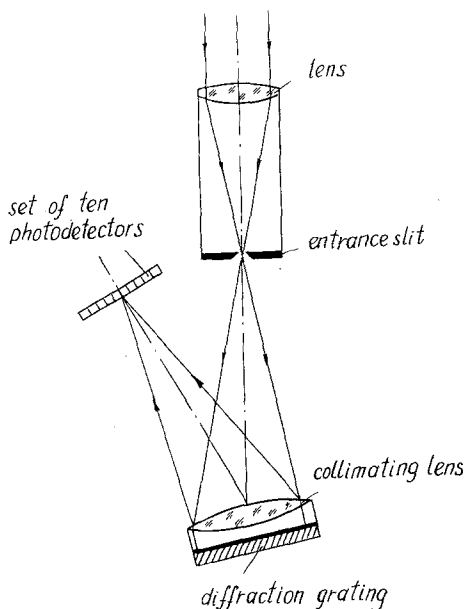


Fig. 4. Schematic diagram of the optical system of the 10-wavelength pyrometer.

### 3. DETERMINATION OF REFLECTIVITY

As stated above, if the sample is irradiated diffusely the measured property is the hemispherical-directional reflectance factor, which, by Helmholtz's reciprocity, is equivalent to the directional-hemispherical reflectance factor. The reflectance factor for hemispherical collection is numerically equal to the reflectance evaluated under the same conditions of irradiation and collection. For measuring the spectral hemispherical-directional reflectance  $\rho_\lambda(2\pi, \theta, \psi, T)$  the flux reflected by the sample is compared to that reflected by a standard of known reflectance. It is computed by use of the equation

$$\rho_\lambda(2\pi, \theta, \psi, T) = \frac{U_i}{U_{s,i}} \rho_{s,\lambda} \quad (1)$$

where  $U_i$  and  $U_{s,i}$  are the signals from the photodetector at  $i$  for sample and standard, respectively, and  $\rho_{s,\lambda}$  is the spectral reflectance of the white standard.

Opal glass and fluorocarbon are used as standard materials in the visible and in the infrared, respectively. They have a high diffuse reflectance

in the spectral range 0.2–2.5  $\mu\text{m}$  (>97%) and their optical properties are accurately known.

In order to provide uniform diffuse irradiation of the sample, the sphere was coated with a pressed layer of high-purity polyfluorocarbon powder that has good reflection properties [6].

#### 4. METHOD

The method for measuring the spectral directional–hemispherical reflectance near high-temperature phase transformations of refractory materials is based on the following assumptions: (a) opacity of the sample, (b) the hypothesis of local thermal equilibrium for the validity of Kirchhoff's law, and (c) the reciprocity principle.

The directional emittance  $\varepsilon_\lambda(\theta, \psi, T)$ , directional–hemispherical reflectance  $\rho_\lambda(\theta, \psi, 2\pi, T)$ , and true temperature  $T$  were computed using the equations

$$\varepsilon_\lambda(\theta, \psi, T) = 1 - \rho_\lambda(\theta, \psi, 2\pi, T) \quad (2)$$

$$\rho_\lambda(\theta, \psi, 2\pi, T) = \rho_\lambda(2\pi, \theta, \psi, T) \quad (3)$$

$$T^{-1} - T_r^{-1} = c_2^{-1} \lambda \ln[1 - \rho_\lambda(2\pi, \theta, \psi, T)] \quad (4)$$

where  $\lambda$  is wavelength,  $c_2$  is Planck's second radiation constant, and  $T_r$  is radiance temperature.

After examining the details of the experiment, the following conclusions were drawn on the assumptions above.

1. The hypothesis of the local thermal equilibrium is quite reliable for sample cooling rates of 2500  $\text{K} \cdot \text{s}^{-1}$  as in the present case.

2. The degree of diffusion and uniformity of the flux incident on the sample is rather high. The deviation from diffuse irradiation made a considerably smaller contribution to the total error than other sources of error. This was verified by measurements of the spectral reflectivities of materials with different surface reflection types. They were polished aluminium and copper (specular reflectance), smoked magnesium oxide and barium sulfate (diffuse reflectance), and opal glass (mixed specular–diffuse reflectance). The results obtained were in agreement with the literature values within the estimated errors.

3. The most critical assumption is the opacity of the sample. The advantage of the present method is the use of a polychromatic reference source, which enables one to use wavelengths where the sample is opaque.

## 5. SOURCES OF UNCERTAINTY

The instability of the flash-lamps and size variations of the air clearance between the lower sphere aperture and the sample surface are the main sources of random uncertainty in the method, while systematic uncertainties stem mainly from the uncertainty in the spectral reflectivity of the white standard, the occurrence of the holes in the integrating sphere wall, and the nonperfectly diffuse irradiation of the sample. Additional sources of uncertainty are related to temperature and wavelength measurements. The evaluation of the listed sources of uncertainty has shown that the overall uncertainty in the reflectivity values measured in the spectral interval 0.4–1.1  $\mu\text{m}$  and in the temperature range 1300–3000 K does not exceed  $\pm 2\%$  at the confidence level of  $P = 0.95$ .

The sample material was samarium oxide, which had a purity better than 99.9%. All the samples were initially heated to temperatures above the melting point in order to produce smooth and reproducible surfaces. It is important to note that for this method it is necessary to use samples of high purity (the impurity content must be less than 0.5%) to avoid errors in the temperature measurement originating from the concentration of the impurities in the center of the sample during cooling.

## 6. EXPERIMENTAL RESULTS AND DISCUSSION

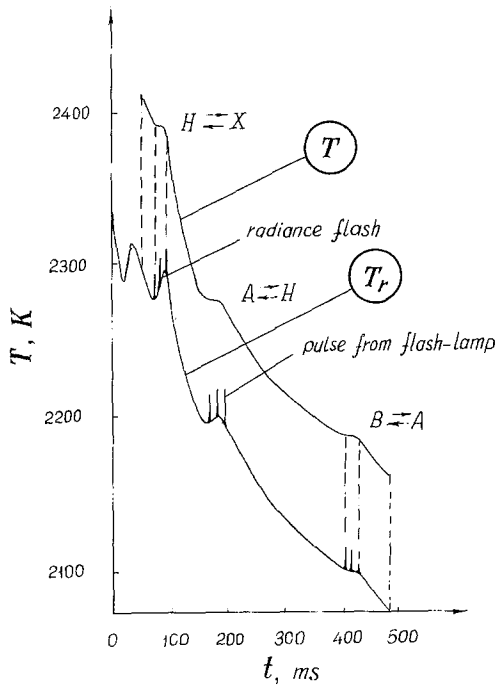
Samarium oxide at high temperatures ( $> 2000$  K) undergoes three polymorphous transformations in the solid state [7]. The transformation temperatures for samarium oxide are given in Table I: A, hexagonal; B, monoclinic; H, hexagonal (high-temperature form); and X, space-centered crystalline modifications of  $\text{Sm}_2\text{O}_3$ , respectively.

Figure 5 shows the radiance temperature at 0.644  $\mu\text{m}$  as a function of the sample cooling time. The curve has four peaks, which correspond to the phase transformations. The radiance flashes revealed as peaks on radiance temperature curve can be related to thermal or optical effects at the phase

**Table I.** Transformation Temperatures (K) of Samarium Oxide above 2000 K<sup>a</sup>

Investigators	B $\rightleftharpoons$ A	A $\rightleftharpoons$ H	H $\rightleftharpoons$ X
Foex and Traverse [7]	2103	2373	2523
Present work	2190 $\pm$ 10	2275 $\pm$ 10	2385 $\pm$ 5

<sup>a</sup> A, hexagonal modification; B, monoclinic modification; H, hexagonal (high-temperature-form) modification; X, space centered crystalline modification.



**Fig. 5.** Radiance temperature at  $0.644 \mu\text{m}$  ( $T_r$ ) and true temperature of  $\text{Sm}_2\text{O}_3$  ( $T$ ) as functions of sample cooling time.

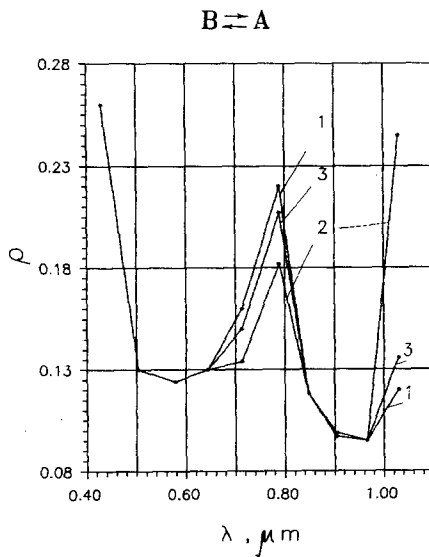


**Fig. 6.** Reflectivity as a function of wavelength near  $A \rightleftharpoons B$  transformation of samarium oxide.



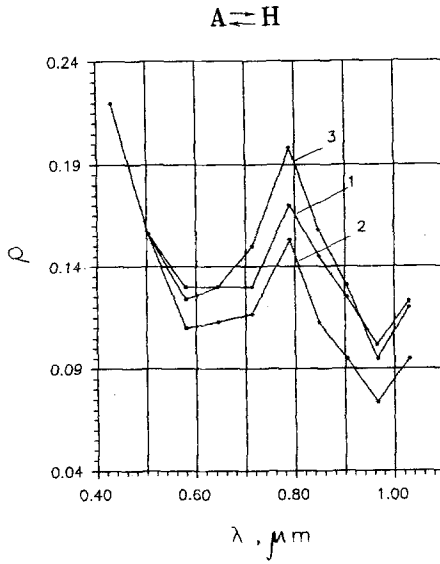


Fig. 7. Reflectivity as a function of wavelength near  $A \rightleftharpoons H$  transformation of samarium oxide.

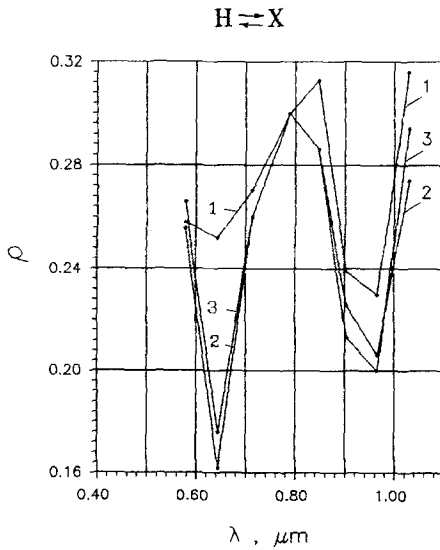


Fig. 8. Reflectivity as a function of wavelength near  $H \rightleftharpoons X$  transformation of samarium oxide.

transitions. The reflectivity measurements near high-temperature transformations (see Figs. 6–8) enable one to partition these contributions for  $\text{Sm}_2\text{O}_3$ . The calculations of the true temperatures show that the plot of the true temperature as a function of time has isothermal parts, expected at phase transitions (see Fig. 5). This may demonstrate that the flashes obtained on curves of the radiance temperature at the phase transitions of  $\text{Sm}_2\text{O}_3$  are of an optical nature. Therefore, we may draw the conclusion that the phase transformations in the solid state are accompanied by light flashes.

The phase transformation temperatures determined from spectral reflectivities at various wavelengths show a reasonably good agreement with the literature values. This tends to confirm the reliability of the method presented in this paper. The results of the measurements of the spectral reflectivities near the phase transformations of other refractory oxides will be reported in future publications.

## REFERENCES

1. M. M. Gurevich, *Photometriya, Teoriya, metoda, i priboru* (Leningrad, 1983), pp. 217–229.
2. F. J. J. Clarke and J. A. Larkin, *High Temp. High Press.* **17**:89 (1985).
3. R. Siegel and J. R. Howell, *Thermal Radiation Heat Transfer* (McGraw-Hill, New York, 1972), Chap. 3.
4. J. C. Richmond, *High Temp. High Pressures* **11**:355 (1979).
5. L. N. Latyev, V. Ya. Chekovskoi, and E. N. Shestakov, *High Temp. High Press.* **2**:175 (1970).
6. K. L. Eckerle, W. H. Venable, Jr., and V. R. Weidner, *J. Appl. Opt.* **15**:703 (1976).
7. M. Foex and J. P. Traverse, *Rev. Int. Hautes Temp. Refract.* **3**:429 (1966).